IBEM-FEM model of the vibratory response of a buried, elastic strip footing

Aldemar P. Siqueira[1], Pérsio L. A. Barros[1], Josué Labaki[1]

[1]*School of Mechanical Engineering, University of Campinas*
200 Mendeleyev St, 13083-860, Campinas SP, Brazil
a235583@dac.unicamp.br, persio@unicamp.br, labaki@unicamp.br

Abstract. This work investigates the dynamic response of an elastic, partially buried strip footing under vertical and horizontal external time-harmonic loads. The footing is modeled as a two-dimensional embedded rectangle discretized by a plane-strain isoparametric finite element. The soil is a two-dimensional, isotropic, viscoelastic half-space modeled through an Indirect-Boundary Element formulation. Solutions for this medium are obtained by superposition of Green's functions for buried loads. Direct kinematic compatibility and equilibrium conditions are used to couple the finite element mesh to the boundary element mesh, assuming perfectly bonded contact at the foundation-soil interface. The effect of foundation embedment and elastic properties on the dynamic behavior of the foundation is illustrated with selected numerical examples.

Keywords: Boundary elements, soil-structure interaction, coupled methods

1 Introduction

The dynamic response of footings resting on or embedded in soil represents an important problem in geotechnical engineering. Considering that many daily structures are supported by long, partially buried footings, understanding how the footing depth of embedment affects its dynamic behavior is crucial in the design of dynamically loaded structures. The foundation stiffness is another essential determinant of the structure's dynamic behavior. Footings often are modeled as rigid, which is an assumption that may be inappropriate in many situations: eg. buildings supported by several individual footings and earth dams (Ai et al. [1], Gutierrez and Chopra [2]).

Over the last decades, the dynamic response of strip footings has been extensively researched and some representative results are presented here. Luco and Westmann [3] studied the vibration of a rigid strip footing bonded to an elastic half-space by using the theory of singular integral equations. Spyrakos and Beskos [4] presented a direct time domain boundary element method-finite element method (BEM-FEM) formulation to investigate the dynamic response of an elastic massless surface footing subjected to external and internal (seismic) excitation. Israil and Ahmad [5] and Ahmad and Bharadwaj [6] investigated the dynamic response of a rigid, massless footing embedded in layered soils through a direct BEM formulation. More recently, Spyrakos and Xu [7] reported a massive, elastic, embedded strip footing model using a FEM-BEM coupling formulation to investigate the effect of footing flexibility, mass and embedment on the foundation dynamic behavior.

This work presents a model of the time-harmonic response of an massive, elastic strip footing embedded in soil. The finite element method is used to model the footing while an indirect formulation of the boundary element method (IBEM) is used to model the isotropic, viscoelastic half-space representing the soil. Perfect bonding between foundation and soil is imposed at the contact interface by assuming direct kinematic compatibility and equilibrium conditions, thus resulting in a IBEM-FEM coupling formulation. The influence of footing stiffness and embedment depth on the dynamic response and contact tractions distribution is investigated.

2 Problem statement

Consider an elastic strip footing of Young's modulus E_f, Poisson's ratio ν_f, mass density ρ_f with infinite length in the y direction, a rectangular cross-section of width $2a$ and height b embedded in a two-dimensional homogeneous, isotropic, viscoelastic half-space of mass density ρ_s, Shear's modulus G_s, Poisson's ratio ν_s and damping ratio β. It is considered a plane strain case and that the structure is perfectly bonded to the soil throughout the structure-soil interface. Time-harmonic horizontal and vertical loads of magnitude F_x and F_z, respectively, can be applied anywhere in the domain of the structure in terms of nodal equivalents.

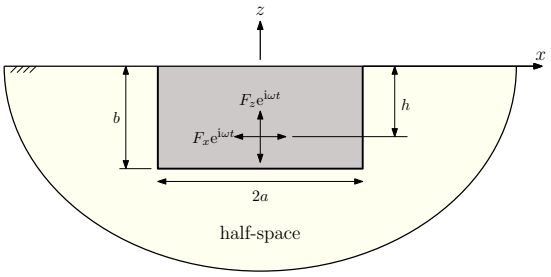

Figure 1. Elastic strip footing embedded in a homogeneous half-space.

3 Formulation

3.1 Model of the Structure

The structure is modeled with linear-elastic, four-noded isoparametric quadrilateral finite elements (FE), with two degrees of freedom per node (displacements in the $x-$ and $z-$ directions). The elemental stiffness and mass matrices are given by (Petyt [8]): $\mathbf{k}_e = \int_{-1}^{+1}\int_{-1}^{+1} \mathbf{B}^T\mathbf{C}\mathbf{B}\det[\mathbf{J}]d\xi d\zeta$, $\mathbf{m}_e = \rho_f \int_{-1}^{+1}\int_{-1}^{+1} \mathbf{N}^T\mathbf{N}d\xi d\zeta$, where $\mathbf{B}$ is the strain-displacement transformation matrix, $\mathbf{C}$ is the constitutive matrix for a plane strain case and $\mathbf{J}$ is the Jacobian operator, $\mathbf{N}$ is the shape function vector, ξ and ζ are the parametric coordinates. The dynamic stiffness matrix of the structure is given by:

$$\bar{\mathbf{K}} = \mathbf{K}_g - \omega^2\mathbf{M}_g, \tag{1}$$

in which $\mathbf{K}_g$ and $\mathbf{M}_g$ are, respectively, the global stiffness and mass matrices of the structure obtained through the classical FE assembly scheme and ω is the applied load frequency.

3.2 Model of the soil

In this work, an Indirect Boundary Element Method formulation is used to model the soil. This procedure consists in connecting the displacement and tractions at discrete points in the half-space through a set of fictitious loads. These loads must satisfy prescribed continuity and equilibrium conditions given at the discrete points.

The soil-foundation contact interface is discretized in N_s constant boundary elements (BE), where $N_s = 2N_v + N_h$, N_v is the number of elements in the side walls ($x = \pm a, -b \leq z \leq 0$) and N_h is the number of elements in the bottom surface ($-a \leq x \leq a, z = -b$). Each BE has a node at its center, on which the displacement and traction values are measured. For the whole interface, the displacements and tractions are given by:

$$\mathbf{u_b} = \mathbf{U}\mathbf{q}, \tag{2}$$

$$\mathbf{t_b} = \mathbf{T}\mathbf{q}, \tag{3}$$

in which $\mathbf{u_b} = \left\{u_x^1 \;\; u_z^1 \;\; u_x^2 \;\; u_z^2 \;\; \dots \;\; u_x^{N_s} \;\; u_z^{N_s}\right\}^T_{2N_s\times 1}$ is the vector of displacements, $\mathbf{t_b} = \left\{t_x^1 \;\; t_z^1 \;\; t_x^2 \;\; t_z^2 \;\; \dots \;\; t_x^{N_s} \;\; t_z^{N_s}\right\}^T_{2N_s\times 1}$, is the corresponding vector of tractions, $\mathbf{q} = \left\{q_x^1 \;\; q_z^1 \;\; q_x^2 \;\; q_z^2 \;\; \dots \;\; q_x^{N_s} \;\; q_z^{N_s}\right\}^T_{2N_s\times 1}$, is the vector of fictitious loads, $\mathbf{U}_{2N_s\times 2N_s}$ and $\mathbf{T}_{2N_s\times 2N_s}$ are, respectively, the matrices of displacement and traction influence functions, which are Green's functions for uniformly distributed loads developed by Barros [9]. The present formulation uses stress and displacement influence functions for time-harmonic loads applied inside the half-space. Each term $u_{r,s}^{i,j}$ and $t_{rs}^{i,j}$ of matrices $\mathbf{U}$ and $\mathbf{T}$ represents, respectively, the displacement and traction of the element i in the $r = x, z$-direction due to a unit fictitious load uniformly distributed over element j in the $s = x, z$-direction. For each i, j pair, submatrices

$$\mathbf{U}^{i,j} = \begin{bmatrix} u_{xx}^{i,j} & u_{xz}^{i,j} \\ u_{zx}^{i,j} & u_{zz}^{i,j} \end{bmatrix}, \tag{4}$$

$$\mathbf{T}^{i,j} = \begin{bmatrix} t_{xx}^{i,j} & t_{xz}^{i,j} \\ t_{zx}^{i,j} & t_{zz}^{i,j} \end{bmatrix}, \tag{5}$$

are used to assemble $\mathbf{U}$ and $\mathbf{T}$. The traction influence functions are given in terms of stress influence functions by $t_{rt}^{i,j} = \sigma_{rst}^{i,j} n_r^i$, $(r, s, t = x, z)$, where $\sigma_{rst}^{i,j}$ is the rs-stress component on i-element due to a load in the t-direction applied at j-element, and n_r^i is the r-component of the vector $\mathbf{n}^i$ normal to the i-element. This vector points outward the material, such that at the bottom surface $\mathbf{n} = (0, 1)$, while $\mathbf{n} = (1, 0)$ and $\mathbf{n} = (-1, 0)$ at the left and right walls, respectively. Influence functions for loads that are uniformly distributed in the vertical direction are used for elements placed at the side walls of the interface, while influence functions for loads that are uniformly distributed in the horizontal direction are used for elements at the bottom wall.

The influence functions mentioned so far are solutions to the stress and displacement fields inside the half-space due to a load applied inside the half-space. These functions can be written as (Barros [9]):

$$u_i(x, z) = \int_0^\infty \bar{u}_i(\lambda, x, z)\bar{p}(\lambda)d\zeta, \tag{6}$$

$$\sigma_{ij}(x, z) = \int_0^\infty \bar{\sigma}_{ij}(\lambda, x, z)\bar{p}(\lambda)d\zeta, \quad i, j = x, z \tag{7}$$

where $\bar{u}_i$ and $\bar{\sigma}_{ij}$ are functions of the elastic constants, the load depth and the frequency, while the terms $\bar{p}$ are the Fourier transform of the applied load. These improper integrals do not have an analytic solution and must be evaluated numerically, which is a quite difficult task because the integrands of eqs. (6) and (7) are characterized with two distinct regions: a portion with the presence of singularities and a portion with an oscillatory-decaying behavior. In the present work, the singularities problem is addressed by incorporating a small hysteretic damping into the material constants, through the elastic-viscoelastic correspondence principle (Christensen [10]): $c_{ij}^* = c_{ij}(1 + \mathrm{i}\beta)$, where $\mathrm{i} = \sqrt{-1}$. This strategy smooths out the singularities and makes them integrable by ordinary adaptive quadratures. The oscillatory portion is evaluated with an adaptive Gaussian quadrature (Piessens et al. [12]). For a detailed discussion of the influence functions and their numeric evaluation see Barros [9].

3.3 IBEM-FEM coupling

The structure is discretized such that there is one finite element coupled to one boundary element at the interface, as illustrated in Fig. 2. Each FE is considered to be perfectly bonded to its corresponding BE. Displacements and tractions are considered uniformly distributed over the elements.

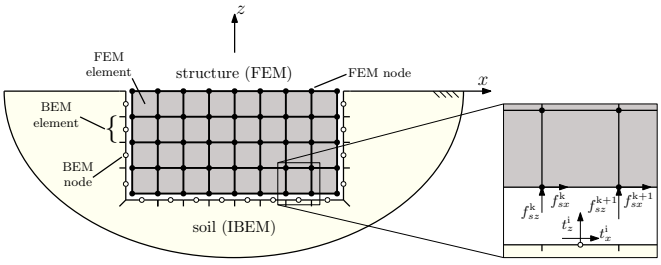

Figure 2. IBEM-FEM coupling scheme for the structure embedded in soil model.

The influence of the presence of the soil is incorporated as a set of equivalent nodal contact forces $\mathbf{f_s}$ acting on the finite elements at the foundation-soil interface. The dynamic equation of motion for the interface is given by: $\bar{\mathbf{K}}\mathbf{u_f} = \mathbf{f} - \mathbf{f_s}$, in which $\bar{\mathbf{K}}$ is the dynamic stiffness matrix, $\mathbf{u_f}$ is the vector of nodal displacements at the interface and $\mathbf{f}$ is the nodal vector of applied external loads. Given that the boundary and finite elements have different orders of approximation, the number of nodes in the BE mesh is incompatible with those of the FE mesh. The vector of contact forces $\mathbf{f_s}$, written in terms of the vector of contact tractions $\mathbf{t_b}$, must account for this difference through the following linear transformation: $\mathbf{f_s} = \mathbf{A}\mathbf{t_b}$, in which $\mathbf{f_s} = \left\{ f^1_{sx} \;\; f^1_{sz} \;\; f^2_{sx} \;\; f^2_{sz} \;\; \cdots \;\; f^{n_n}_{sx} \;\; f^{n_n}_{sz} \right\}^T_{2n_n \times 1}$,

$$\mathbf{A} = \frac{1}{2}\begin{bmatrix}
{}^v l_e^1 & 0 & & & \cdots & & & & & \\
0 & {}^v l_e^1 & & & \cdots & & & & & \\
 & & & & \cdots & & & & {}^v l_e^{N_h} & 0 \\
 & & & & \cdots & & & & 0 & {}^v l_e^{N_h} \\
{}^v l_e^1 & 0 & {}^v l_e^{N_h+1} & 0 & \cdots & & & & & \\
0 & {}^v l_e^1 & 0 & {}^v l_e^{N_h+1} & \cdots & & & & & \\
 & & & \ddots & & & {}^v l_e^{2N_h} & 0 & {}^v l_e^{N_h} & 0 \\
 & & & & & & 0 & {}^v l_e^{2N_h} & 0 & {}^v l_e^{N_h} \\
 & & & & & \iddots & & & & \\
{}^v l_e^{N^*} & 0 & {}^h l_e^{N^*} & 0 & & & & & & \\
0 & {}^v l_e^{N^*} & 0 & {}^h l_e^{N^*} & & & & & & \\
 & & {}^h l_e^{N^*} & 0 & & & & & & \\
 & & 0 & {}^h l_e^{N^*} & & & & & & \\
 & & & & \ddots\;\ddots & & & & & \\
 & & & & & {}^h l_e^{N} & 0 & & & \\
 & & & & & 0 & {}^h l_e^{N} & & & \\
 & & & & & {}^h l_e^{N} & 0 & {}^v l_e^{N} & 0 & \\
 & & & & & 0 & {}^h l_e^{N} & 0 & {}^v l_e^{N} &
\end{bmatrix}_{2n_n \times 2n_s}, \tag{8}$$

where ${}^v l_e$ is the height of the finite elements along the side walls, ${}^h l_e$ is the width of the finite elements at the bottom surface, $N = 2N_v + N_h - 2$ is the total number of finite elements at the interface, $n_n = N + 3$ and $n_s = N + 2$ are the number of nodes in the FE and BE interface meshes, respectively, and $N^* = N - N_h + 1$. In view of this compatibilization, the equilibrium equation for the structure nodes at the interface can be written as: $\bar{\mathbf{K}}\mathbf{u_f} + \mathbf{A}\mathbf{T}\mathbf{q} = \mathbf{f}$.

In order to impose kinematic compatibility between the soil and the structure, the displacement of each BE must be written in terms of its corresponding FE equivalent nodal displacements. This can be obtained by $\mathbf{u_b} = \mathbf{D}\mathbf{u_f}$, in which

$$\mathbf{D} = \frac{1}{2}\begin{bmatrix}
1^1 & 0 & & & 1^1 & 0 & & & & & & \\
0 & 1^1 & & & 0 & 1^1 & & & & & & \\
 & & & & 1^{N_h+1} & 0 & & & & & & \\
 & & & & 0 & 1^{Nh_1} & & & & & & \\
 & & & & & & \ddots & 1^{N^*} & 0 & & & \\
 & & & & & & & 0 & 1^{N^*} & & & \\
 & & & & & & & 1^{N^*} & 0 & 1^{N^*} & 0 & \\
 & & & & & & & 0 & 1^{N^*} & 0 & 1^{N^*} & \\
\vdots & \vdots & \vdots & \vdots & \vdots & \vdots & & & & \ddots\;\ddots & & \\
 & & & & & & & & 1^N & 0 & 1^N & 0 \\
 & & & & & & & & 0 & 1^N & 0 & 1^N \\
 & & & & & & & & & & 1^N & 0 \\
 & & & & & & \iddots & & & & 0 & 1^N \\
 & & & & & 1^{2N_h} & 0 & & & & & \\
 & & & & & 0 & 1^{2N_h} & & & & & \\
 & & 1^{N_h} & 0 & & 1^{N_h} & 0 & & & & & \\
 & & 0 & 1^{N_h} & & 0 & 1^{N_h} & & & & &
\end{bmatrix}_{2n_s \times 2n_n}. \tag{9}$$

This compatibilization yields $\mathbf{D}\mathbf{u_f} - \mathbf{U}\mathbf{q} = \mathbf{0}$, which results in the equilibrium equation at the soil-structure

interface:

$$\begin{bmatrix} \bar{\mathbf{K}} & \mathbf{AT} \\ \mathbf{D} & -\mathbf{U} \end{bmatrix} \begin{Bmatrix} \mathbf{u_f} \\ \mathbf{q} \end{Bmatrix} = \begin{Bmatrix} \mathbf{f} \\ \mathbf{0} \end{Bmatrix}. \tag{10}$$

Assembling the terms in eq. (10) corresponding to the interface into the system for the full structure yields

$$\left[\begin{array}{c|c} \bar{\mathbf{K}} & \begin{matrix} \mathbf{AT} \\ \mathbf{0} \end{matrix} \\ \hline \begin{matrix} \mathbf{D} & \mathbf{0} \end{matrix} & -\mathbf{U} \end{array}\right] \left\{\begin{array}{c} \mathbf{u_f} \\ \hline \mathbf{q} \end{array}\right\} = \left\{\begin{array}{c} \mathbf{f} \\ \hline \mathbf{0} \end{array}\right\}, \tag{11}$$

in which the zeros correspond to the degrees of freedom inside and at the top surface of the structure. The solution of this system yields the displacements on nodes of the structure and the fictitious contact loads applied to the BE at the interface. Displacement and stress solutions can be obtained anywhere in the soil domain by post-processing from the vector of fictitious loads (Carneiro et al. [13]).

4 Numerical results

This section presents an analysis of the influence of an elastic strip footing stiffness and embedment depth on the dynamic response and contact tractions distribution at the foundation-soil interface. Results are presented in terms of the normalized frequency $a_0 = \omega a\sqrt{\rho_s/G_s}$ and the nondimensional horizontal and vertical compliances $c^*_{ii} = aG_s u_i/F_i,\ (i = x, z)$, in which u_i is the displacement measured at the centroid of the cross section. All results consider a footing with $\nu_f = 0.3$ and the soil as an isotropic half-space with $\nu_s = 0.33$ and $\eta = 0.05$. In order to validate the present model, Fig. 3 and Fig. 4 show, respectively, the vertical and horizontal compliances of a rigid, massless embedded footing. Different embedment ratios b/a were considered, including that of a surface footing ($b/a = 0$), approximated with the present model by setting $b = 0.01a$. Rigid and massless properties can be obtained with the present model by making the structure much stiffer than the soil ($E_f = 10^6 E_s$) and with zero mass density ($\rho_f = 0$). These results were compared with Israil and Ahmad [5] and Ahmad and Bharadwaj [6] showing a good agreement.

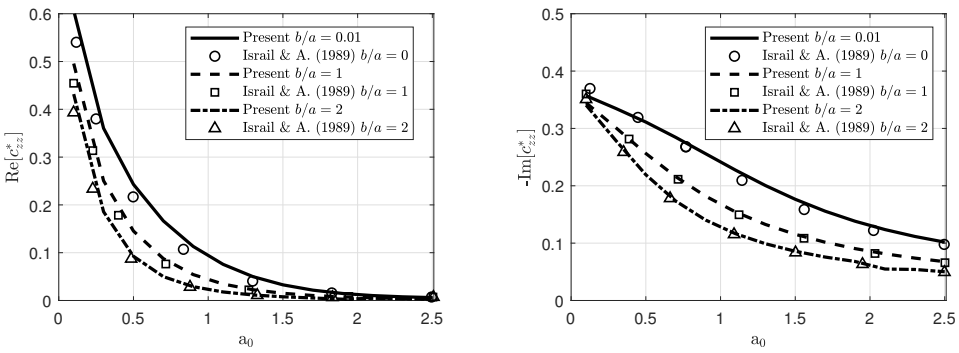

Figure 3. Vertical response.

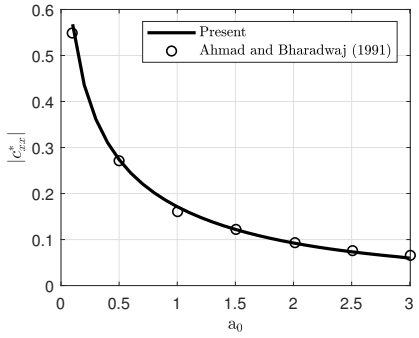

Figure 4. Horizontal response $(b/a = 1)$.

Figure 5 shows the influence of the soil-structure stiffness ratio E_s/E_f on dynamic response of a massless embedded footing $(b/a = 1)$. In these results, the external loads are applied at a depth of h over the centroid of the cross-section (Fig. 1). It can be noticed that stiffer foundations present significantly smaller kinematic responses. Notice that for values of $E_s/E_f < 10^{-2}$, the foundation behaves like a rigid body.

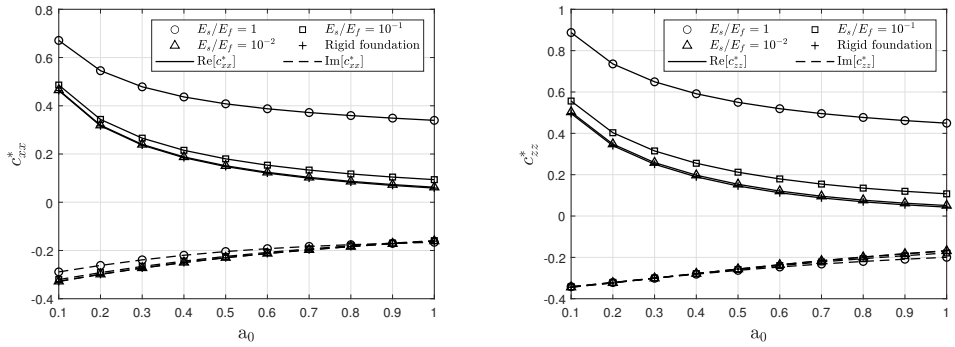

Figure 5. Influence of stiffness ratio on dynamic response $(b/a = 1)$.

Figure 6 shows the effect depth of embedment of the footing on its dynamic behavior, for different values of stiffness ratio. This example considers a footing with $\rho_f = 2\rho_s$ and applied load with $a_0 = 1$. Notice that, as the embedment ratio increases, the amplitude of the foundation's dynamic response drastically decreases, specially for stiffer foundations, and for values of $b/a > 1$, the influence of the depth of embedment of the footing on its dynamic response becomes negligible.

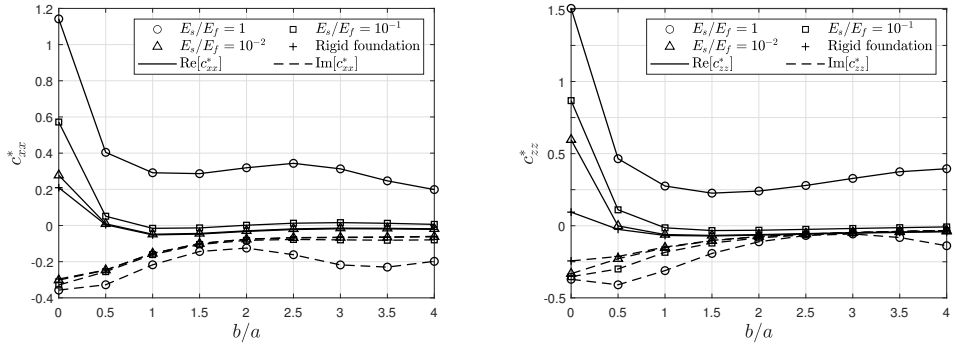

Figure 6. Influence of embedment ratio on dynamic response.

Figure 7 presents the influence of the depth of embedment of a rigid footing on the distribution of contact tractions at the bottom soil-structure interface. This analysis considers a footing with $\rho_f = 2\rho_s$ and applied load

with $a_0 = 1$. The results are presented in terms of the normalized traction components $t^{i*}_{jk} = 2at^i_{jk}/F_k$ $(j, k = x, z)$ acting at the interface between the bottom of the footing and the soil. Notice that the amplitude of tractions decrease significantly with increase of embedment ratio, specially for foundations subjected to vertical loads. The sharp increase in the magnitude of the traction components toward the edge of the foundation ($x/a \rightarrow 1$) is physically consistent.

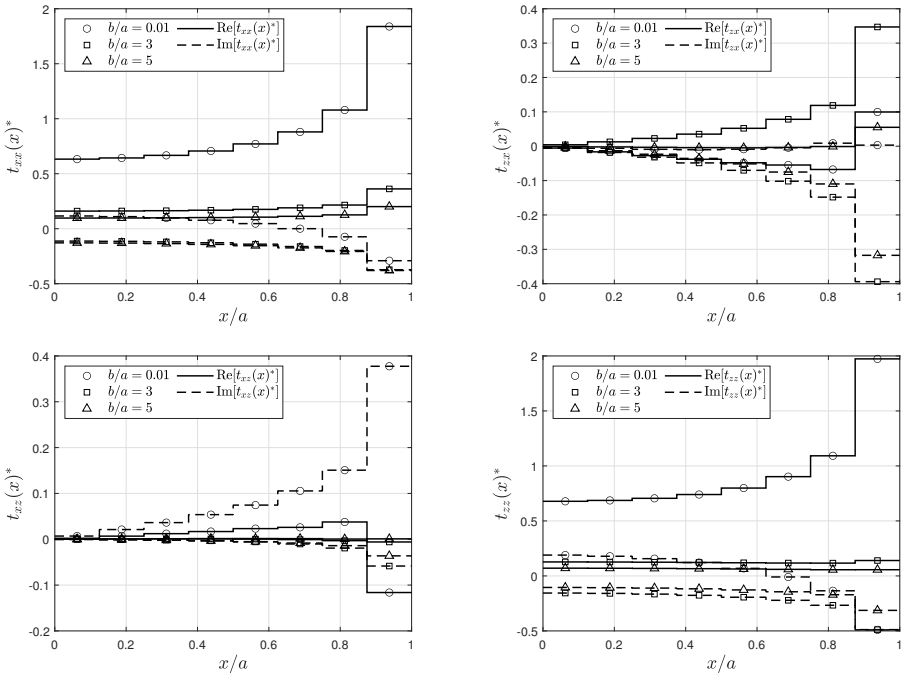

Figure 7. Influence of embedment ratio on contact tractions distribution (rigid foundation).

5 Conclusions

This paper presented a model of the time-harmonic response of an infinite elastic strip footing partially buried in soil and subjected to external loads. An IBEM-FEM coupling scheme was proposed to model foundation-soil interaction. Perfect bonding between structure and soil was obtained by establishing kinematic compatibility and equilibrium conditions throughout soil-foundation interface. Results showed that elastic properties and depth of embedment of the foundation significantly affect its dynamic response.

Authorship statement. The authors are the only responsible for the printed material included in this paper.

References

[1] Z. Y. Ai, H. T. Li, and Y. F. Zhang. Vertical vibration of a massless flexible strip footing bonded to a transversely isotropic multilayered half-plane. *Soil Dynamics and Earthquake Engineering*, vol. 92, pp. 528–536, 2017.
[2] J. A. Gutierrez and A. K. Chopra. A substructure method for earthquake analysis of structures including structure-soil interaction. *Earthquake Engineering & Structural Dynamics*, vol. 6, n. 1, pp. 51–69, 1978.
[3] J. Luco and R. A. Westmann. Dynamic response of a rigid footing bonded to an elastic half space. vol. , 1972.
[4] C. Spyrakos and D. Beskos. Dynamic response of flexible strip-foundations by boundary and finite elements. *Soil dynamics and earthquake engineering*, vol. 5, n. 2, pp. 84–96, 1986.
[5] A. Israil and S. Ahmad. Dynamic vertical compliance of strip foundations in layered soils. *Earthquake engineering & structural dynamics*, vol. 18, n. 7, pp. 933–950, 1989.
[6] S. Ahmad and A. Bharadwaj. Horizontal impedance of embedded strip foundations in layered soil. *Journal of geotechnical engineering*, vol. 117, n. 7, pp. 1021–1041, 1991.
[7] C. Spyrakos and C. Xu. Dynamic analysis of flexible massive strip–foundations embedded in layered soils by hybrid bem–fem. *Computers & structures*, vol. 82, n. 29-30, pp. 2541–2550, 2004.
[8] M. Petyt. *Introduction to finite element vibration analysis*. Cambridge university press, 2010.

[9] P. L. A. Barros. *Elastodinâmica de meios transversalmente isotrópicos: Funções de Green e o Método dos Elementos de Contorno na análise da interação solo-estrutura (Elastodynamics of Transversely Isotropic Media: Green's Functions and Boundary Element Method Analysis of the Soil-Structure Interaction)*. PhD thesis, University of Campinas, Campinas, Brazil, 1997.
[10] R. Christensen. *Theory of viscoelasticity*. Academic Press, 1982.
[11] de P. L. Almeida Barros, J. Labaki, and E. Mesquita. Ibem-fem model of a piled plate within a transversely isotropic half-space. *Engineering Analysis with Boundary Elements*, vol. 101, pp. 281–296, 2019.
[12] R. Piessens, de E. Doncker-Kapenga, C. W. Überhuber, and D. K. Kahaner. *Quadpack: a subroutine package for automatic integration*, volume 1. Springer Science & Business Media, 2012.
[13] D. A. S. Carneiro, J. Labaki, S. S. Hoefel, and P. L. A. Barros. Dynamic displacement and strain fields within trenched soils: Post-processing quantities from indirect-bem's fictitious loads. In *XL Iberian Latin American Congress on Computacional Methods in Engineering*, Natal,Rio Grande do Norte, Brazil, 2019.